JOURNAL OF SOLID STATE CHEMISTRY 3, 197–205 (1971)

Phase Relations of $CsClO_4$ and $CsBF_4$ to High Pressures

P. W. RICHTER AND CARL W. F. T. PISTORIUS

Chemical Physics Group of the National Physical and National Chemical Research Laboratories, South African Council for Scientific and Industrial Research, Pretoria, South Africa

Received September 28, 1970

Orthorhombic $CsBF_4$ III transforms at 159.1°C to cubic $CsBF_4$ II, space group *Fm3m*, with $a_0 = 7.859$ Å at 230°C. The high-pressure phase diagrams of $CsClO_4$ and $CsBF_4$ were studied by means of differential thermal analysis and volumetric techniques, and found to be closely similar to those of $RbClO_4$ and $RbBF_4$. All the new phases previously predicted for $CsBF_4$ actually appeared. Entropy calculations confirmed the earlier suggestion that the entropy change of the $RbBF_4$ I/IV, $CsClO_4$ II/I and $CsBF_4$ II/I transitions approximately equals $R\ln 8$.

Introduction

The high-pressure polymorphism of the univalent perchlorates was first studied by Bridgman (*1*) to 50 kbar and ~100°C. There have been recent studies of the complete phase diagrams to 40 kbar of $NaBF_4$, $NaClO_4$ (*2*), $KClO_4$, KBF_4 (*3*), $RbClO_4$ and $RbBF_4$ (*4*).

The room temperature modifications $CsClO_4$ III and $CsBF_4$ III have the barite structure (*5*, *6*), and are therefore isostructural with the corresponding modifications of the potassium, thallium and rubidium salts (*7*), as well as with $NaClO_4$ III and $NaBF_4$ IV (*2*). These substances have cubic high-temperature modifications (*7*) with the space group *Fm3m* (*2*). The disorder in the structure is not caused by free rotation of the anions, but is of a type which maximizes the cation–oxygen (or cation–fluorine) distances. This transition occurs at 220°C (*8*, *9*) in the case of $CsClO_4$, but has not yet been observed for $CsBF_4$ although it was predicted (*4*) to occur below ~250°C at atmospheric pressure. In the cases of KBF_4 (*3*) and $RbBF_4$ (*4*) this high-temperature phase undergoes yet another transition at high pressures and temperature to a modification which was suggested (*4*), on the basis of entropy considerations, also to be cubic, space group *Fm3m*, with probably the anti-NH_4Cl I structure (*10*, *11*). Pistorius and Clark (*4*) predicted a similar phase to occur in the phase diagram of $CsBF_4$. In the phase diagram of $RbBF_4$ yet another phase $RbBF_4$ V appears below the melting curve at still higher pressures and temperatures. This phase may possibly have the 16F atoms of the tetramolecular unit-cell uniformly distributed on four spheres centered at the 4(a) positions of *Fm3m* (*4*). A similar phase was expected (*4*) to occur in the phase diagram of $CsBF_4$. Bridgman (*1*) found that $RbClO_4$, $TlClO_4$, NH_4ClO_4, and $CsClO_4$ have high-pressure transitions to denser forms, and it was predicted (*4*) that $CsBF_4$ will have a high-pressure transition near ~2 kbar similar to that of $CsClO_4$. $CsBF_4$ melts at 550°C (*12*) and $CsClO_4$ at 570°C (*9*), in both cases with decomposition.

Experimental

$CsClO_4$ with a purity of 99+% was obtained from Electronic Space Products, Inc. $CsBF_4$ was prepared by precipitation from aqueous solutions of Hopkin and Williams HBF_4 and 99% pure Cs_2CO_3 obtained from Koch–Light, washing with water and ethanol, and drying at 200°C.

Pressures up to 55 kbar were generated in a piston–cylinder device (*13*). The arrangement proposed by Haygarth and Kennedy (*14*) was used for pressures above 40 kbar. The furnace assembly was similar to that used by Cohen et al. (*15*). Phase changes were detected by means of differential thermal analysis (DTA), using Chromel–Alumel thermocouples. The results were corrected for the effect of pressure on the thermocouples (*16*). The samples were contained in metal capsules which incorporated thermocouple wells (*17*). The work on $CsBF_4$ was done in Cu capsules, while Ni capsules were used for $CsClO_4$. No capsule attack was observed. The axial thermal gradient along the sample capsule was reduced by sandwiching the capsule between two insulated metal plugs (*18*). Typical DTA signals are shown in Fig. 1. Each phase boundary was based on several separate runs. The results of different runs were consistent. The heating/cooling rate was in the range 0.2–1.0°C/sec.

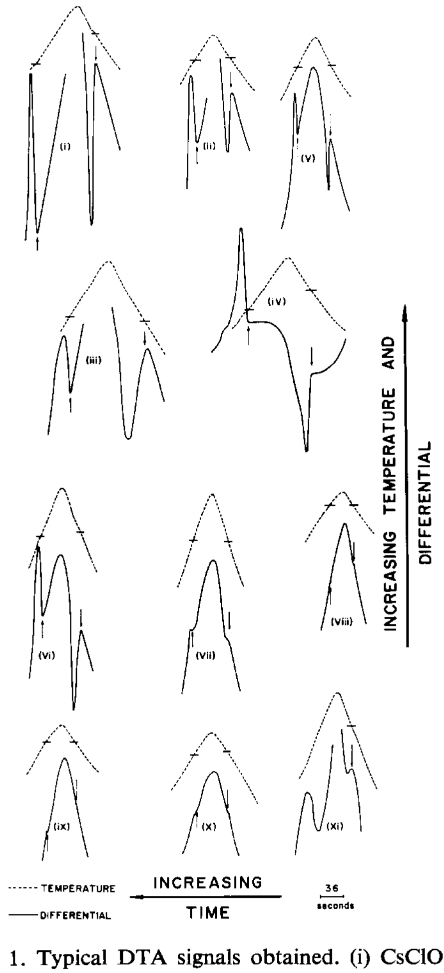

FIG. 1. Typical DTA signals obtained. (i) $CsClO_4$ III/II at 0 kbar, 220.8°C heating, 196.8°C cooling; (ii) $CsClO_4$ II/I at 6.4 kbar, 419.8°C heating, 417.6°C cooling; (iii) $CsClO_4$ IV/I at 17.1 kbar, 539.6°C heating, 544.8°C cooling; (iv) $CsBF_4$ III/II at 0 kbar, 168.2°C heating, 150.8°C cooling; (v) $CsBF_4$ II/I at 6.0 kbar, 398.0°C heating, 397.2°C cooling; (vi) $CsBF_4$ IV/I at 41.2 kbar, 646.2°C heating, 637.7°C cooling; (vii) $CsBF_4$ I/liq at 5.0 kbar, 635.6°C; (viii) $CsBF_4$ I/V at 12.5 kbar, 662.8°C heating, 662.5°C cooling; (ix) $CsBF_4$ I/VI at 23.7 kbar, 657.5°C heating, 656.7°C cooling; (x) $CsBF_4$ VI/V at 22.6 kbar, 729.3°C heating, 727.5°C cooling; (xi) $CsBF_4$ V/liq at 13.7 kbar, 898.3°C.

Sliding friction was determined by comparing results obtained on increasing and on decreasing pressure. The pressures obtained in this way were further corrected for the effect of nonsymmetrical pressure losses (*19*). The final pressures are expected to be in error to less than 0.5 kbar. Phase boundaries were taken to be the mean of heating and cooling in the case of solid–solid transitions, but only melting temperatures were plotted in the case of solid–liquid phase changes.

High-pressure polymorphism was studied by precompressing ~10 g of sample wrapped in thin lead foil. The walls of the pressure vessel were coated with Molykote to minimize friction. Fillers of talc and a stopper of unfired pyrophyllite were used at the upper end of the bore of the pressure vessel to prevent extrusion of the sample when pressure was applied. The displacement of the piston was measured as a function of pressure, using a dial gauge readable to 0.003 mm. A transition could be recognized by inspecting the plot of piston displacement against load. Piston rotation (*20*) was used to further minimize friction at a transition. Temperatures above room temperature could be obtained by wrapping a heating coil around the pressure plate.

Crystallography

The X-ray powder diffraction pattern of $CsBF_4$ at 230°C was measured, using filtered CuK_α radiation. The sample was contained in a sealed Lindemann tube mounted in a Weissenberg camera, and heated by means of a stream of hot nitrogen. Temperature was measured by a thermocouple junction ~0.5 mm from the sample. The measurements were calibrated by photographing the powder pattern of pure CaF_2 standard at 25°C on the same film.

The diffraction pattern of $CsBF_4$ at 230°C was totally different from that at 25°C, but similar to that of $RbBF_4$ I at 229°C (*4*), and showed the presence of a phase transition between 25°C and 230°C. The powder pattern of this phase, designated as $CsBF_4$ II, at 230°C is shown in Table I. All the observed peaks could be assigned on the basis of an fcc unit-cell with $a_0 = 7.859 \pm 0.010$ Å, as compared with $a_0 = 7.990$ Å in the case of $CsClO_4$ II (*9*).

Results

Cesium Perchlorate

The phase diagram of $CsClO_4$ is shown in Fig. 2. The III/II transition yielded strong and sharp

TABLE I

POWDER PATTERN OF $CsBF_4$ II AT 230°C(CuK_α RADIATION)

d_{obsd} (Å)	d_{calcd} (Å)	hkl	I
4.5	4.537	111	m
3.924	3.928	200	vvs
2.768	2.779	220	m
2.359	2.370	311	m
2.267	2.268	222	w
1.802	1.803	331	w
1.756	1.757	420	w
1.606	1.604	422	w
1.511	1.512	333	m

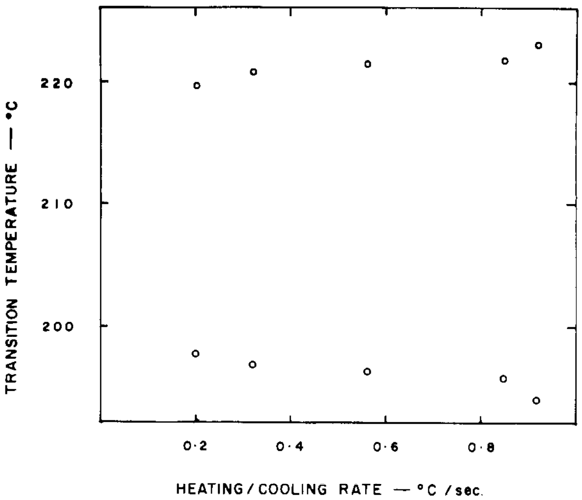

FIG. 3. Dependence on the rate of heating and cooling of the $CsClO_4$ III/II transition temperature at atmospheric pressure. Upper curve, heating; lower curve, cooling.

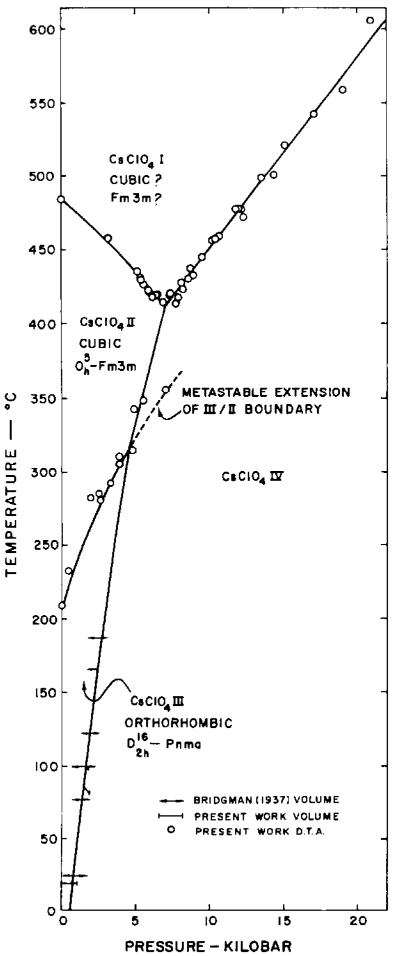

FIG. 2. Phase diagram of $CsClO_4$ at 24 kbar.

DTA signals at atmospheric pressure [Fig. 1(i)] with ~25° thermal hysteresis. A plot of the transition temperature as a function of heating/cooling rate (Fig. 3) indicates that the thermal hysteresis is only slightly dependent on the heating/cooling rate in the range 0.2–0.9°C/sec. The mean of the III → II and II → III transition temperatures is essentially independent of the heating/cooling rate. The present atmospheric-pressure mean transition point is 209.2 ± 0.5°C, being the average of twelve determinations. The earlier values (219–220°C) in the literature clearly refer only to the III → II transition. At higher pressures the signals become considerably broader. This is a consequence of the steep slope of the transition line and the large volume change (see below) associated with the transition, which cause a considerable local change in pressure as the transition occurs, and thereby broaden the DTA signals. The $CsClO_4$ III/IV transition line, previously studied by Bridgman (*1*), meets the III/II transition line at a triple point $CsClO_4$ II/IV/III at 4.5 kbar, 314°C. A weak DTA signal on the metastable extension of the III/II transition line was observed ~2.5 kbar beyond the triple point upon increasing pressure in one run. This shows that the III/IV transition does not become markedly less sluggish at elevated temperatures.

The resulting $CsClO_4$ IV/II transition line rises steeply to the I/IV/II triple point at 7 kbar, 411°C, where a new phase $CsClO_4$ I appears. The DTA signals due to the II/I transition were sharp [Fig. 1(ii)] near the I/IV/III triple point, with less than ~2°C hysteresis. At lower pressures, however, the hysteresis increased to ~5°C at 5 kbar. Broad DTA signals were encountered at atmospheric pressure and 485°C, and these are ascribed to the II/I

TABLE II

TRANSITION PRESSURES AFTER PISTON ROTATION

Transition line	Upstroke Pressure (kbar)	Downstroke Pressure (kbar)	Temp. (°C)
$CsClO_4$ III/IV	1.076	0.001	19.5
	1.835	—	82.5
	—	1.458	86.0
	1.740	—	99.0
	—	1.664	101.0
$CsBF_4$ III/IV	2.079	1.403	23.2
	2.991	2.879	83.0
	3.382	3.230	107.0

transition. The signals due to the IV/I transition were strong and sharp [Fig. 1(iii)]. In some runs the cooling temperatures on this transition line were higher than the heating temperatures. This was ascribed to a local pressure increase due to the volume increase upon transition. The IV/I transition line was followed to 21 kbar, where the sample decomposed at 633°C.

An attempt was made to obtain the melting point of $CsClO_4$ I in a closed sample capsule at atmospheric pressure. However, decomposition started at 523°C, well before the melting point near ~570°C (*9*) was reached.

Piston-displacement and piston-rotation techniques were used to determine three points on the $CsClO_4$ III/IV phase boundary. It was possible to reduce the pressure uncertainty to values well below those obtained by Bridgman (*1*). The transition pressures obtained by means of piston rotation are given in Table II. The agreement with Bridgman's results is excellent. It was found that the transition remained slow at higher temperatures, although the "region of indifference" became negligible. The phase relations of $CsClO_4$ are summarized in Table III.

TABLE III

PHASE RELATIONS OF $CsClO_4$ AND $CsBF_4$

Transition line	Fit	Standard deviation
$CsClO_4$ III/II	$t(°C) = 209.2 + 31.7P - 1.70P^2$	0.4 kbar
$CsClO_4$ III/IV	$P = 0.55 + 0.0098t + 0.0000085t^2$	0.18 kbar
$CsClO_4$ II/IV	$t(°C) = 314 + 39(P - 4.5)$	0.2 kbar
$CsClO_4$ II/I	$t(°C) = 485 - 8.55P - 0.286P^2$	2.3°C
$CsClO_4$ IV/I	$t(°C) = 411 + 13.1(P - 7.0)$	5.3°C
$CsBF_4$ III/II	$t(°C) = 159.1 + 38.3P - 2.53P^2$	4.1°C
$CsBF_4$ III/IV	$P = 1.308 + 0.0179t$	0.012 kbar
$CsBF_4$ II/IV	$t(°C) = 302 + 38(P - 6.6)$	—
$CsBF_4$ II/I	$t(°C) = 450 - 1.06P - 1.238P^2$	1.4°C
$CsBF_4$ IV/I	$t(°C) = 359 + 11.46(P - 8.1) - 0.131(P - 8.1)^2 + 0.0013(P - 8.1)^3$	1.5°C
$CsBF_4$ IV/VI	$t(°C) = 651 + 5.92(P - 42.5)$	0.8°C
$CsBF_4$ I/VI	$t(°C) = 670.5 - 2.15(P - 16.6) + 0.053(P - 16.6)^2$	1.4°C
$CsBF_4$ I/V	$t(°C) = 635.5 + 5.45(P - 5.0) - 0.219(P - 5.0)^2$	1.5°C
$CsBF_4$ VI/V	$t(°C) = 670.5 + 9.75(P - 16.6) - 0.073(P - 16.6)^2$	2.3°C
$CsBF_4$ I/liq	$P/2.088 = (T/831.8)^{13.94} - 1$	0.7°C
$CsBF_4$ V/liq	$P/1.636 = (T/908.7)^{7.351} - 1$	5.6°C

Triple point	Pressure (kbar)[a]	Temperature (°C)[a]
$CsClO_4$ IV/III/II	4.5	314
$CsClO_4$ I/IV/II	7.0	411
$CsBF_4$ IV/III/II	6.6	302
$CsBF_4$ I/IV/II	8.1	359
$CsBF_4$ V/I/liq	5.0	635.5
$CsBF_4$ VI/I/V	16.6	670.5
$CsBF_4$ VI/IV/I	~42.5	~651

[a] The uncertainties corresponding to these values are best judged from Figs. 2 and 4.

The heat effect associated with the $CsClO_4$ III/II transition was measured by using a Perkin–Elmer differential scanning calorimeter Model 1B. The entropy of the transition was found to be

$$\Delta S_{III/II} = 15.4 \pm 0.7 \text{ J/deg mole} \approx R \ln 8.$$

With the present initial slope of 31.7°C/kbar the Clapeyron relation yields

$$\Delta V_{III/II} = 4.9 \text{ cm}^3\text{/mole}$$

which is ~7.1% of the molar volume of $CsClO_4$ III.

According to Bridgman (*1*)

$$\Delta V_{IV/III} = 3.6 \text{ cm}^3\text{/mole}$$

in the temperature range 120–190°C. Using the mean slope of the III/IV transition line in this temperature range, viz., 82°C/kbar, the Clapeyron equation yields

$$\Delta S_{IV/III} = 4.4 \text{ J/deg mole.}$$

If the assumption is made that $\Delta S_{IV/III}$ and $\Delta S_{III/II}$ remain approximately constant along the respective transition lines, it follows that

$$\Delta S_{IV/II} = 19.8 \text{ J/deg mole,}$$

and therefore, using the slope of the $CsClO_4$ IV/II transition line,

$$(\Delta V_{IV/II})_{P=4.5\text{ kbar}} = 7.7 \text{ cm}^3\text{/mole.}$$

If it is assumed that $\Delta S_{II/I}$ equals $R\ln 8$ as in the case of the corresponding $RbBF_4$ I/IV transition (*4*), the slope of the $CsClO_4$ II/I transition line at the I/IV/II triple point, viz., –12.5°C/kbar, yields

$$(\Delta V_{II/I})_{P=7\text{ kbar}} \simeq -2.2 \text{ cm}^3\text{/mole.}$$

By summation, therefore,

$$\Delta S_{IV/I} \simeq 37 \text{ J/deg mole,}$$

and since the initial slope of the $CsClO_4$ IV/I phase boundary is 13.1°C/kbar,

$$(\Delta V_{IV/I})_{P=7\text{ kbar}} \simeq 4.9 \text{ cm}^3\text{/mole,}$$

and by summation

$$(\Delta V_{IV/II})_{P=7\text{ kbar}} \simeq 7.1 \text{ cm}^3\text{/mole,}$$

in excellent agreement with the value at the $CsClO_4$ IV/III/II triple point. These calculations are quite sensitive to the value assumed for $\Delta S_{II/I}$, and therefore shows that $\Delta S_{II/I}$ is actually quite close to $R\ln 8$ as expected.

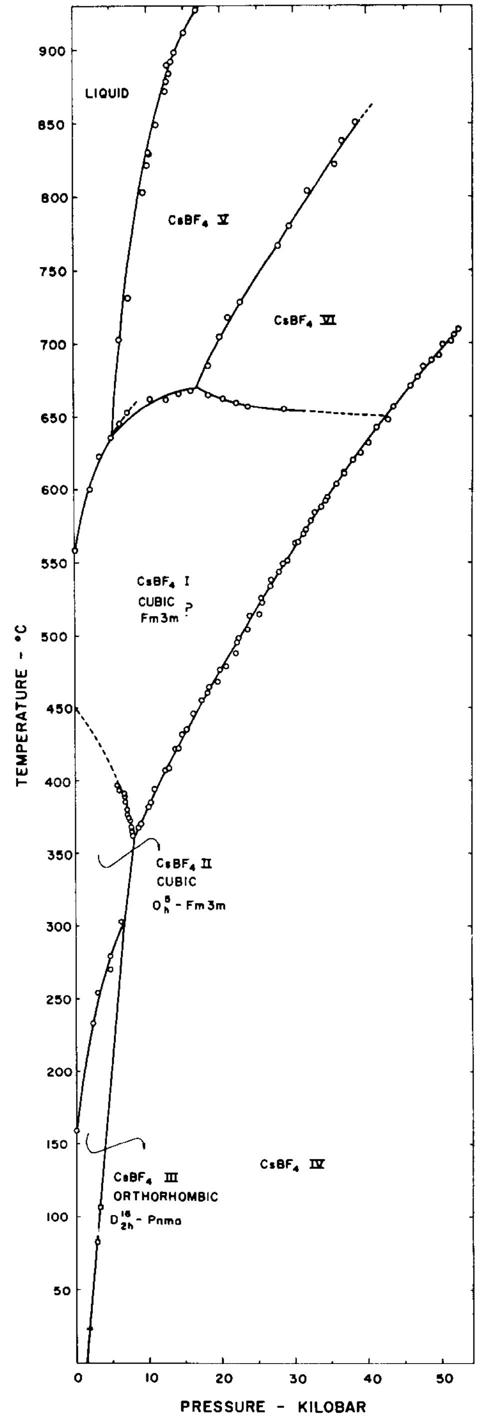

FIG. 4. Phase diagram of $CsBF_4$ to 53 kbar.

Cesium Tetrafluoroborate

The phase diagram of $CsBF_4$ is shown in Fig. 4. The expected $CsBF_4$ III/IV transition was easily observed by means of piston-displacement techniques. A typical curve of piston displacement versus load is shown in Fig. 5. The volume change was 2.9 cm³/mole, closely similar to that of the corresponding $CsClO_4$ III/IV transition, viz., 3.6 cm³/

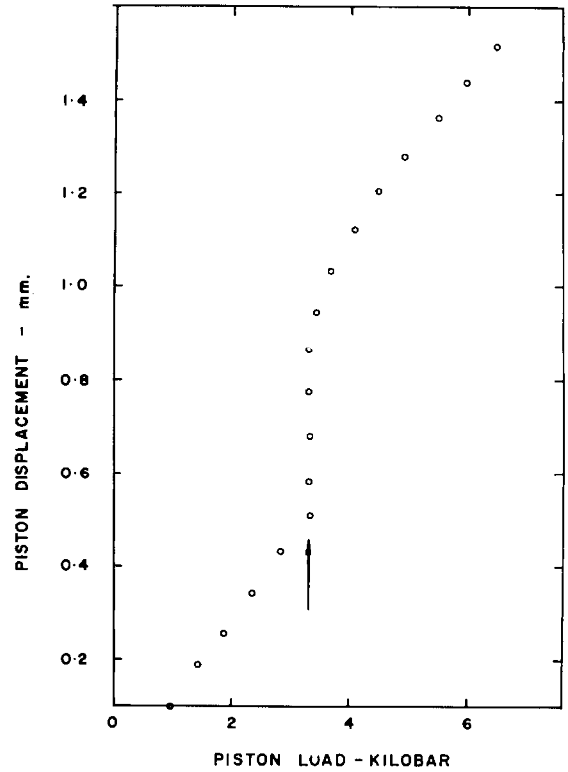

FIG. 5. Curve of upstroke piston displacement versus piston load for $CsBF_4$ at 23.2°C, showing the new III/IV transition.

mole (*1*). The $CsBF_4$ III/IV transition was extremely sharp, and excellent values of the transition pressures could be obtained by means of piston rotation. The transition line rises with temperature from 1.74 ± 0.34 kbar at 23.2°C to 3.306 ± 0.076 kbar at 107°C. The transition pressures obtained are listed in Table II.

The $CsBF_4$ III/II transition, which was first shown to occur between 25°C and 230°C by means of crystallographic methods above, yielded very strong and sharp DTA signals at atmospheric pressure [Fig. 1(iv)]. The ~17°C thermal hysteresis was essentially independent of heating/cooling rates in the range 0.15–0.9°C/sec, as is shown in Fig. 6. The atmospheric pressure transition point is 159.1 ± 0.5°C, being the mean of twelve determinations. The transition signals at higher pressures did not broaden to the same extent as in the case of $CsClO_4$. The $CsBF_4$ III/II transition line meets the III/IV transition line at a triple point IV/III/II at 6.6 kbar, 302°C. The resulting IV/II transition line did not yield detectable DTA signals. However, it is terminated at the $CsBF_4$ I/IV/II triple point at 8.1 kbar, 359°C with the appearance of a new phase $CsBF_4$ I. The DTA signals due to the II/I transition were sharp and strong [Fig. 1(v)] with ~5°C thermal hysteresis. As was the case for the corresponding transition of $CsClO_4$, the $CsBF_4$ II/I transition becomes sluggish at low pressures, and could not be followed below ~5.8 kbar. Extrapolation of the phase boundary suggests that it will occur at ~450°C at atmospheric pressure. The $CsBF_4$ IV/I transition yielded sharp and considerably stronger DTA signals [Fig. 1(vi)]. In some runs the signals obtained on cooling were located at higher temperatures than those obtained on heating. This was ascribed to the local pressure increase on the sample due to the volume increase of the IV → I transformation. The $CsBF_4$ IV/I transition line rises steeply with pressure to the IV/I/VI triple point at 42.5 kbar, 651°C.

The melting point of $CsBF_4$ I was encountered at 559°C at atmospheric pressure. The DTA signals obtained along this melting curve were weak

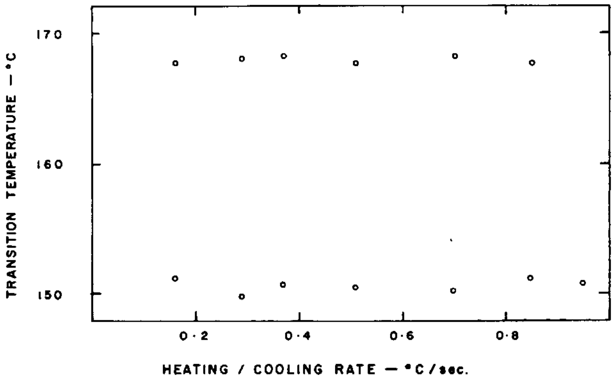

FIG. 6. Dependence on the rate of heating and cooling of the $CsBF_4$ III/II transition temperature at atmospheric pressure. Upper curve, heating; lower curve, cooling.

[Fig. 1(vii)]. The melting curve of $CsBF_4$ I rises steeply, but with considerable curvature, to the $CsBF_4$ V/I/liquid triple point at 5 kbar, 635.5°C, where a new phase $CsBF_4$ V appears. Several points on the metastable extrapolation of the melting curve of $CsBF_4$ I were obtained. The melting curve of $CsBF_4$ V rises very steeply with pressure, and was followed to 16.6 kbar, 927°C. It yielded DTA signals which were considerably better-defined [Fig. 1(xi)] than those due to the melting of $CsBF_4$ I. The I/V transition yielded extremely weak, but nevertheless sharp, DTA signals [Fig. 1(viii)] with less than 0.5°C thermal hysteresis. The transition line rises with pressure to the $CsBF_4$ V/VI/I triple point at 16.6 kbar, 670.5°C, where yet another new phase $CsBF_4$ VI appears. The resulting $CsBF_4$ VI/V transition also yielded extremely faint DTA signals [Fig. 1(x)] with less than 0.5°C thermal hysteresis. The transition line rises with pressure, and was followed to 38.4 kbar, 850°C. The DTA signals due to the I/VI transition were weak but sharp [Fig. 1(ix)], with no observable hysteresis. This transition line falls slightly with pressure, and has abnormal curvature. It could not be directly observed beyond ~30 kbar, but the slope of the IV/I transition line changes rather abruptly from 7.05°C/kbar to 5.92°C/kbar at ~42.5 kbar, ~651°C. This point is considered to be the $CsBF_4$ VI/IV/I triple point. The signals due to the IV/VI transition were not markedly different from those due to the IV/I transition. The IV/VI transition line is linear to 52 kbar, 710°C.

The phase relations of $CsBF_4$ are summarized in Table III. The melting curves were fitted to the Simon equation.

The entropy of the $CsBF_4$ III/II transition, as measured by using a Perkin–Elmer differential scanning calorimeter, is

$$\Delta S_{\mathrm{III/II}} = 17.5\ \mathrm{J/deg\ mole} \approx R\ln 8.$$

With the present initial slope of 38.3°C/kbar the Clapeyron relation yields

$$\Delta V_{\mathrm{III/II}} = 6.7\ \mathrm{cm^3/mole}$$

which is ~10% of the molar volume of $CsBF_4$ III. The comparison value derived from diffraction data is

$$\Delta V_{\mathrm{III/II}} = 8.6\ \mathrm{cm^3/mole},$$

but this value includes the thermal expansion from 25–230°C, and is therefore merely an upper limit.

From the observed volume change at the $CsBF_4$ III/IV transition, viz., 2.9 cm³/mole, and the slope of the transition line, viz., 56°C/kbar, the Clapeyron relation yields

$$\Delta S_{\mathrm{IV/III}} = 5.1\ \mathrm{J/deg\ mole}.$$

If the assumption is made that $\Delta S_{\mathrm{IV/III}}$ and $\Delta S_{\mathrm{III/II}}$ remain approximately constant along the respective transition lines, it follows that

$$\Delta S_{\mathrm{IV/II}} = 22.6\ \mathrm{J/deg\ mole},$$

and therefore, using the slope of the $CsBF_4$ IV/II transition line,

$$(\Delta V_{\mathrm{IV/II}})_{P=6.6\,\mathrm{kbar}} = 8.6\ \mathrm{cm^3/mole}.$$

In the case of $RbBF_4$ (*4*) it was shown that the entropy of the $RbBF_4$ I/IV transition, which corresponds to the present $CsBF_4$ II/I transition, was $R\ln 8$. Taking this also to be the entropy of the $CsBF_4$ II/I transition, and using the slope of the $CsBF_4$ II/I transition line at the I/IV/II triple point, viz., –20.8°C/kbar, we find that

$$\Delta V_{\mathrm{II/I}} \simeq -3.6\ \mathrm{cm^3/mole}.$$

The entropy change $\Delta S_{\mathrm{IV/I}}$ must equal the sum of $\Delta S_{\mathrm{IV/II}}$ and $\Delta S_{\mathrm{II/I}}$, therefore

$$\Delta S_{\mathrm{IV/I}} \simeq 40\ \mathrm{J/deg\ mole}$$

and since the initial slope of the $CsBF_4$ IV/I transition line is 11.5°C/kbar,

$$(\Delta V_{\mathrm{IV/I}})_{P=8.1\,\mathrm{kbar}} \simeq 4.6\ \mathrm{cm^3/mole}.$$

$\Delta V_{\mathrm{IV/II}}$ at the I/IV/II triple point equals the sum of $\Delta V_{\mathrm{IV/I}}$ and $\Delta V_{\mathrm{I/II}}$, therefore

$$(\Delta V_{\mathrm{IV/II}})_{P=8.1\,\mathrm{kbar}} \simeq 8.2\ \mathrm{cm^3/mole},$$

in excellent agreement with the value obtained at the IV/III/II triple point, viz., 8.6 cm³/mole. These calculations are quite sensitive to the value assumed for $\Delta S_{\mathrm{II/I}}$, and therefore shows that $\Delta S_{\mathrm{II/I}}$ is actually quite close to $R\ln 8$ as expected.

At the $CsBF_4$ VI/IV/I triple point the slope of the I/VI transition line is nearly zero, and $\Delta V_{\mathrm{I/VI}}$ is therefore nearly zero. Assuming $\Delta S_{\mathrm{IV/I}}$ to be ~40 J/deg mole at this point, and using the slope 7.05°C/kbar of the IV/I transition line,

$$(\Delta V_{\mathrm{IV/I}})_{P=42.5\,\mathrm{kbar}} \simeq 2.8\ \mathrm{cm^3/mole},$$

and also

$$(\Delta V_{\mathrm{IV/VI}})_{P=42.5\,\mathrm{kbar}} \simeq 2.8\ \mathrm{cm^3/mole}.$$

The slope of the IV/VI transition line is 5.9°C/kbar, so that

$$\Delta S_{\mathrm{IV/VI}} \simeq 47\ \mathrm{J/deg\ mole}$$

and therefore

$$\Delta S_{\mathrm{I/VI}} \simeq 7\ \mathrm{J/deg\ mole}.$$

This value depends largely on the difference between the slopes of the IV/I and IV/VI transition lines at the VI/IV/I triple point, and cannot be considered as better than order-of-magnitude. However, it does show that free three-dimensional rotation of the anion tetrahedra cannot occur in $CsBF_4$ VI, since this would require an entropy gain of ~80 J/deg mole (*21*). It is not possible to carry out similar calculations on the entropy of $CsBF_4$ V at this stage.

Discussion

The phase diagrams of $CsClO_4$ and $CsBF_4$ are strikingly similar. In particular, the slopes as well as, where determined, the volume and entropy changes of the pairs of III/IV, III/II, IV/II, II/I and IV/I transition lines are closely the same in both cases, and it can be confidently assumed that the corresponding phases are isostructural for these substances. Furthermore, a comparison with previous work (*2–4*) shows that $CsBF_4$ IV and $CsClO_4$ IV can be expected to have the same structure as $RbBF_4$ III and $RbClO_4$ III, while $CsBF_4$ I and $CsClO_4$ I can be expected to have the same structure as $RbBF_4$ IV and KBF_4 III. It is not certain which of $CsBF_4$ V or VI is similar to $RbBF_4$ V.

It was previously (*4*) suggested, on the basis of the relative strengths of the DTA signals for the $RbBF_4$ III/I and I/IV transitions, that the entropy change for the $RbBF_4$ I/IV transition is close to $R\ln 8$. Since DTA signal strength in a high-pressure environment is a poor indicator of latent heat, this suggestion was not fully convincing. Sufficient data were available for $CsClO_4$ and $CsBF_4$ to enable a calculation of ΔS for the II/I transitions (which correspond to the $RbBF_4$ I/IV transition), and the previous suggestion was found to be correct. This partly confirms the proposed structure (*4*) for $RbBF_4$ IV, $CsBF_4$ I, $CsClO_4$ I and KBF_4 III, i.e. one in which four F atoms (one from each tetrahedron) are distributed in the 24(e) positions of the space group *Fm3m*, while the other 12F atoms are uniformly distributed around 24 circles centered at 24(e). This proposed model involves one-dimensional rotation of the anion tetrahedra about cell diagonals, as in the case of the high-temperature forms of the ammonium halides (*10*, *11*).

This phase occurs at atmospheric pressure and elevated temperatures in the cases of $CsClO_4$ and $CsBF_4$. If decomposition can be avoided this fact may provide an opportunity for finally confirming the proposed structure by means of high-temperature X-ray diffraction.

It was tentatively suggested (*4*) that free three-dimensional rotation of the anion tetrahedra may occur in the case of $RbBF_4$ V. The corresponding phase of $CsBF_4$ is either V or VI. Approximate entropy calculations show that $CsBF_4$ VI, at any rate, does not have a sufficiently large entropy for free anion rotation.

The high-pressure transitions $RbBF_4$ II/III and $RbClO_4$ II/III occur near ~15 kbar (*4*). No corresponding transitions occur in the potassium salts to 40 kbar (*3*). The corresponding $CsBF_4$ and $CsClO_4$ III/IV transitions occur near ~1 kbar. This suggests the same dependence of transition pressure on cationic radius as found for the *Fm3m*/*Pm3m* transition of the alkali halides, viz., that a large cationic radius simulates higher pressure.

Four of the five new phases here found for $CsBF_4$ have previously been predicted by analogy with the phase diagrams of KBF_4 and $RbBF_4$ (*4*). Such a close correspondence between empirical prediction and the actual state of affairs suggests that a simple theoretical model could possibly explain all the apparently complex polymorphic phenomena encountered in the univalent perchlorates and tetrafluoroborates.

The atmospheric-pressure melting point of $CsBF_4$ I is given as 550°C in the literature (*12*). Our present value for material contained in a metal capsule is 559°C. The discrepancy is smaller than for $NaBF_4$ (*2*), KBF_4 (*3*) or $RbBF_4$ (*4*), and is probably due to slow decomposition of the uncontained material as the temperature was raised to the melting point. If this is correct, the present value should be preferred.

The phase boundaries $CsBF_4$ I/V, I/VI and VI/V are based on extremely weak DTA signals, and cannot be considered to be established beyond possible doubt. However, their existence appears to be confirmed by the various triple points in the high-temperature region.

Acknowledgments

The authors would like to thank Martha C. Pistorius for writing the computer programs used in fitting the data, and Dr. J. C. A. Boeyens for valuable discussions. J. Erasmus and his staff and A. de Kleyn and his staff kept the equipment in good repair, and were responsible for the manufacture of the furnace parts. Calculations were carried out on the IBM System 360/65 H of the National Research Institute for Mathematical Sciences. The DSC studies were carried out by S. Pretorius of the S.A. Coal, Oil and Gas Corporation, Ltd.

References

1. P. W. Bridgman, *Proc. Amer. Acad. Arts Sci.* **72**, 45 (1937).

2. C. W. F. T. Pistorius, J. C. A. Boeyens, and J. B. Clark, *High Temp. High Press.* **1**, 41 (1969).
3. C. W. F. T. Pistorius, *J. Phys. Chem. Solids* **31**, 385 (1970).
4. C. W. F. T. Pistorius and J. B. Clark, *High Temp. High Press.* **1**, 561 (1969).
5. W. Büssem and K. Herrmann, *Z. Kristallogr.* **67**, 405 (1928).
6. L. J. Klinkenberg, *Rec. Trav. Chim. Pays bas* **56**, 36 (1937).
7. R. W. G. Wyckoff, "Crystal Structures," Vol. 3, pp. 45–58, Interscience, New York, 1965.
8. K. Herrmann and W. Ilge, *Z. Kristallogr.* **75**, 41 (1930).
9. B. Kanellakopulos, *J. Inorg. Nucl. Chem.* **28**, 813 (1966).
10. H. A. Levy and S. W. Peterson, *J. Amer. Chem. Soc.* **75**, 1536 (1953).
11. R. Plumb and D. Hornig, *J. Chem. Phys.* **21**, 366 (1953).
12. J. H. de Boer and J. A. M. van Liempt, *Rec. Trav. Chim. Pays bas* **46**, 124 (1927).
13. G. C. Kennedy and P. N. LaMori, *in* "Progress in Very High Pressure Research," (F. P. Bundy, W. R. Hibbard and H. M. Strong, eds.), p. 304, John Wiley, New York, 1961.
14. J. Haygarth and G. C. Kennedy, *Rev. Sci. Instrum.* **38**, 1590 (1967).
15. L. H. Cohen, W. Klement, Jr., and G. C. Kennedy, *J. Phys. Chem. Solids* **27**, 179 (1966).
16. R. E. Hanneman and H. M. Strong, *J. Appl. Phys.* **36**, 523 (1965); **37**, 612 (1966).
17. C. W. F. T. Pistorius, *J. Phys. Chem. Solids* **26**, 1543 (1965).
18. E. Rapoport, *J. Chem. Phys.* **45**, 2721 (1966).
19. C. W. F. T. Pistorius, E. Rapoport, and J. B. Clark, *Rev. Sci. Instrum.* **38**, 1741 (1967).
20. C. W. F. T. Pistorius, *J. Phys. Chem. Solids* **26**, 1003 (1965).
21. G. J. Janz and D. W. James, *Electrochim. Acta* **7**, 427 (1962).